Journal of Inflammation Research

Dovepress
open access to scientific and medical research

Open Access Full Text Article

ORIGINAL RESEARCH

Serum Amyloid A 4 as a Common Marker of Persistent Inflammation in Patients with Neovascular Age-Related Macular Degeneration and Polypoidal Choroidal Vasculopathy

Qingyan Liu[1,2,*], Shuo Sun[1,*], Zhengwei Yang[1,*], Yan Shao[1], Xiaorong Li[1]

[1]Tianjin Key Laboratory of Retinal Functions and Diseases, Tianjin Branch of National Clinical Research Center for Ocular Disease, Eye Institute and School of Optometry, Tianjin Medical University Eye Hospital, Tianjin, 300384, People's Republic of China; [2]Department of Ophthalmology, Anhui NO.2 Provincial People's hospital, Hefei, 230041, People's Republic of China

*These authors contributed equally to this work

Correspondence: Yan Shao; Xiaorong Li, Email 13820179302@163.com; xiaorli@163.com

Background: Neovascular age-related macular degeneration (nAMD) and its subtype, polypoidal choroidal vasculopathy (PCV), are common choroidal vasculopathies. Although they share many common clinical manifestations and treatment strategies, a lack of comprehensive analysis of these conditions means that it is difficult for researchers to further explore the common pathomechanisms of nAMD and PCV. The aim of this study was to characterize aqueous humor (AH) proteome alterations and identify a novel biomarker related to both nAMD and PCV.

Methods: Liquid Chromatography with tandem mass spectrometry (LC-MS/MS) was adopted to analyze the AH proteomes of nAMD, PCV and controls. The target protein was validated using the enzyme-linked immunosorbent assay (ELISA) and subjected to receiver operating characteristic (ROC) curve analysis.

Results: A total of 737 different proteins were identified in all the groups, of which 544 were quantifiable. The bioinformatics analysis suggested that immune response activation is the essential event in both nAMD and PCV. Serum amyloid A (SAA) 4 is closely associated with a number of chronic inflammatory diseases, and it was enriched as the hub protein. ROC analysis showed that SAA4 could distinguish both nAMD and PCV from the controls.

Conclusion: This comprehensive study provides insights into, and furthers our understanding of, the pathological mechanism of nAMD and PCV. Additionally, the SAA4 level alteration may serve as a common biomarker of nAMD and PCV.

Keywords: serum amyloid A 4, inflammation, neovascular age-related macular degeneration, polypoidal choroidal vasculopathy

Introduction

Age-related macular degeneration (AMD) is the leading cause of severe vision loss among elderly people worldwide.[1] The projected number of patients with AMD was 196 million in 2020 and is expected to increase to 288 million in 2040.[2] Many AMD risk factors have been identified, including aging, smoking, genetics and some environmental factors. AMD can be classified into the early, intermediate and late stages. A small number of medium-sized drusen and/or pigment changes can be found in early-stage AMD.[3] As the disease progresses, some AMD patients develop from the early stage to the late stage. There are two types of late-stage AMD: geographic atrophy (GA) and neovascular AMD (nAMD). At its worst, late AMD can cause irreversible vision loss.[4] nAMD is characterized by choroidal neovascularization (CNV), which can lead to vascular leakage, macular edema and subretinal fibrosis accompanied by vision loss.[5] The branching vascular network (BVN), with polyp-like aneurysmal lesions, is a defining characteristic of polypoidal choroidal vasculopathy (PCV), which can be detected by indocyanine green angiography (ICGA) and optical coherence tomography angiography (OCTA). Some studies support the

Received: 20 April 2023
Accepted: 22 August 2023
Published: 29 August 2023

notion that PCV is a subtype of nAMD due to the many similarities between PCV and nAMD, including their pathologies, manifestations and, most importantly, the fact that they both fall into the category of choroidal vasculopathy.[6,7] In recent years, researchers have found that inflammation plays an essential role in the pathogenesis of both nAMD and PCV. Several inflammatory factors are involved in the progress of these diseases.[8,9] Vascular endothelial growth factor (VEGF) is an important stimulator of CNV development. Intravitreal injection of anti-VEGF agents is one of the promising treatments for choroidal vasculopathy.[10] However, the standard treatment is still limited by certain issues, such as a high treatment burden, increased risk of developing subretinal fibrosis, GA development and the fact that nearly 30% of patients have a poor or non-response to the standardized treatment.[11–13] Today, Efdamrofusp alfa, a bispecific fusion protein, can enhance the efficacy of anti-VEGF monotherapies for nAMD patients owing to its targeting of both C3b/C4b and VEGF.[14] Other inhibitors of inflammatory factors, including Interleukin (IL)-1β, IL-6 and IL-8, have also been demonstrated to have deleterious effects on angiogenesis.[15–17] Although these new advances in choroidal vasculopathy mentioned above represent a promising approach, the future direction of choroidal vasculopathy treatment exploration should aim to identify a factor that can inhibit both VEGF and inflammatory factors.

Serum amyloid A (SAA), an acute phase protein, is closely related to many chronic inflammatory diseases. Human SAA proteins have two sub-families: acute phase SAA1 and SAA2, which can trigger the immune cells, and the constitutive SAA4.[18,19] SAA not only promotes tube formation due to an increase in VEGF receptor 2 expression[20] but also induces the expression of inflammatory cytokines and chemokines, including IL-1b, Tumor necrosis factor-α, IL-6 and IL-8, as a result of the chemotaxis of phagocytes.[21] An increased SAA4 protein level is typically detected in response to various inflammatory disorders.[22,23] Seok and Mun both found that circulating SAA4 levels were increased in the serum of patients with rheumatoid arthritis (RA),[24] suggesting that SAA4 might be a novel diagnostic biomarker for RA.[25] Although several functions have been attributed to SAA4 thus far, its predominant role in nAMD and PCV remains unclear. Here, we report a proteomic study on the aqueous humor (AH) of patients with cataracts, nAMD and PCV using label-free quantitative proteomics (Figure 1). Comprehensive analysis of the proteomes demonstrated several enriched pathways, including immunity and inflammation, which had close relationships with both nAMD and PCV. This study provides novel insight into the molecular mechanisms involved in the pathogenesis of nAMD and PCV and its development, and essential data were generated for the identification of more effective treatment strategies by comparing the similarities and differences between nAMD and PCV.

Materials and Methods

Subjects

The Tianjin Medical University Eye Hospital Institutional Review Board approved this study, which conformed with the declaration of Helsinki. Written informed consent was obtained from the patient(s) to publish this paper. In total, 30 subjects, who were divided into 3 groups, were recruited for LC-MS/MS analysis at Tianjin Medical University Eye Hospital, including (Table 1) 10 patients with cataracts (control), 10 treatment-naive patients with nAMD and 10

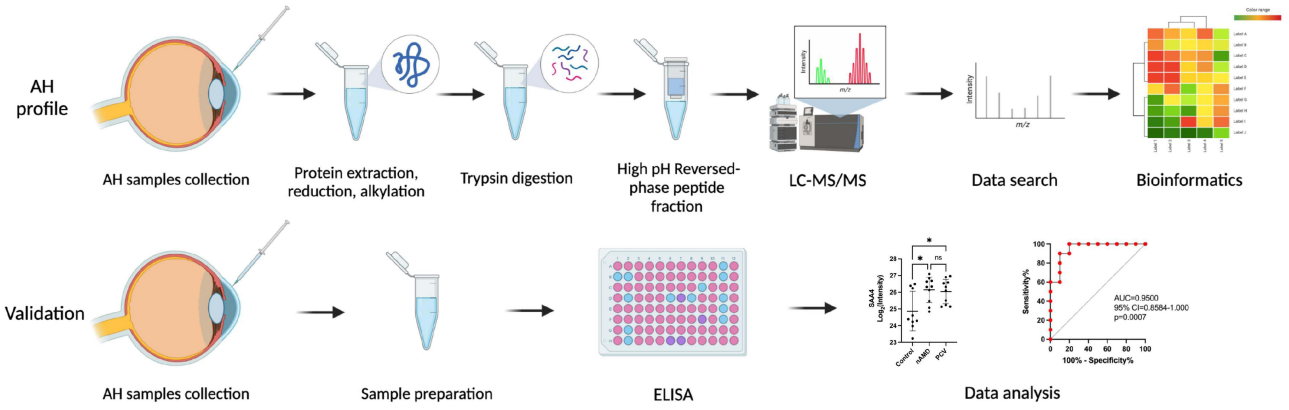

Figure 1 Workflow of the AH proteome profile analysis and the validation of DEPs in nAMD and PCV.

Table 1 Significantly Upregulated Proteins for Each Patient Group

Protein ID	Gene Name	Description	Peptides	FC	p-value
Control vs nAMD					
P29401	TKT	Transketolase	16	3.3	0.035
P01706	IGLV2-11	Immunoglobulin lambda variable 2–11	4	2.9	0.014
P08571	CD14	Monocyte differentiation antigen CD14	8	2.2	0.000
P07585	DCN	Decorin	10	2.2	0.018
P01599	IGKV1-17	Immunoglobulin kappa variable 1–17	3	2.1	0.024
P02675	FGB	Fibrinogen beta chain	24	2.0	0.027
P02753	RBP4	Retinol-binding protein 4	8	2.0	0.002
P35542	SAA4	Serum amyloid A-4 protein	3	2.0	0.023
P07357	C8A	Complement component C8 alpha chain	15	2.0	0.006
P07360	C8G	Complement component C8 gamma chain	9	2.0	0.004
Control vs PCV					
P01706	IGLV2-11	Immunoglobulin lambda variable 2–11	4	3.0	0.006
P01861	IGHG4	Immunoglobulin heavy constant gamma 4	14	2.5	0.036
A0A0B4J1V0	IGHV3-15	Immunoglobulin heavy variable 3–15	2	2.1	0.001
P07360	C8G	Complement component C8 gamma chain	9	1.9	0.018
P08571	CD14	Monocyte differentiation antigen CD14	8	1.9	0.027
Q15223	NECTIN1	Nectin-1	2	1.9	0.045
P07357	C8A	Complement C8 alpha chain	15	1.9	0.041
P35542	SAA4	Serum amyloid A-4 protein	3	1.8	0.044
P00734	F2	Prothrombin	29	1.8	0.008
P00748	F12	Coagulation factor XII	11	1.8	0.026
nAMD vs PCV					
Q06033	ITIH3	Inter-alpha-trypsin inhibitor heavy chain H3	6	2.5	0.035

treatment-naive patients with PCV. All patients with PCV and nAMD in our study were diagnosed specifically with fluorescein angiography (FA) and indocyanine green angiography (ICGA) combined with optical coherence tomography (OCT). The inclusion criteria for nAMD included age over 50 years and a diagnosis of nAMD according to the Age-Related Eye Disease Studies (AREDS) criteria. Patients with nAMD showed classic or occult CNV with FA, with no clusters of polypoidal dilation of the vessels in ICGA. By comparison, the diagnostic test to differentiate PCV from nAMD was mainly based on ICGA to detect the polypoidal lesions with or without presence of a BVN. The controls were recruited from patients with grade 2 or 3 nuclear sclerotic cataracts undergoing surgery. The exclusion criteria for all patients included systemic disease; systemic or ocular infectious disease; the use of systemic corticosteroids, immunosuppressants, or antimetabolites; and other ocular diseases, such as pathological myopia, proliferative diabetic retinopathy, glaucoma, retinal vascular occlusion, and so on. The detailed clinical information is shown in Table 1. There were no statistically significant differences in gender ($p = 0.866$) or age ($p = 0.796$) between these groups.

Sample Collection and Preparation

After topical anesthesia, a mean volume of 100μL of AH sample was obtained at the beginning of cataract surgery or after the intravitreal injection of anti-VEGF agents using an insulin syringe with a 30-gauge needle at the limbus. Thereafter, all AH samples were stored in liquid nitrogen.

All samples were disrupted in SDT lysis buffer (4% sodium dodecyl sulfate (SDS), 100 mM dithiothreitol (DTT), 150 mM Tris-HCl pH 8.0). The filtrate was quantified with the BCA Protein Assay Kit (Bio-Rad, USA). Additionally, protein digestion was carried out according to the filter-aided sample preparation (FASP) procedure. In short, 200 μg of protein (for each sample) was mixed with 30 μL of SDT buffer. Uric acid (UA) buffer (8 M urea, 150 mM Tris-HCl pH 8.0) was used to remove the detergent, DTT and other low-molecular-weight components. Repeated ultrafiltration (Microcon units, 10 kD) was used to deplete the highly abundant proteins. Subsequently, to block the reduced cysteine residues, 100 μL of iodoacetamide (100 mM IAA in UA buffer) was added into mixture. After 30 min of incubation in dark, the filters were washed with UA buffer and 25mM NH_4HCO_3 buffer in sequence. A total of 4 μg of trypsin (Promega, Madison, WI, USA) in 40 μL of 25mM NH_4HCO_3 buffer was applied to ensure the digestion of the suspensions overnight at 37 °C. The resulting peptides were desalted on C18 Cartridges (Empore™ SPE, Sigma, St. Louis, MO, USA). After concentration, they were dissolved in 40 μL of 0.1% formic acid. To estimate the peptide concentration, UV light spectroscopy was applied to measure the absorbance at 280 nm using an extinction coefficient of 1.1 of 0.1% (g/l) solution.

LC-MS/MS Analysis

A Q Exactive mass spectrometer (MS) (Thermo Scientific, Waltham, MA, USA) coupled with Easy nLC (Proxeon Biosystems, now Thermo Fisher Scientific, Waltham, MA, USA) was used for comprehensive LC-MS/MS analysis. The prepared peptides were first loaded into a Thermo Scientific Acclaim trap column (100 μm*2 cm, nanoViper C18, Thermo Scientific, Waltham, MA, USA), with the Thermo Scientific C18-reversed phase analytical column (10 cm long, 75 μm inner diameter, 3μm resin, Thermo Scientific, Waltham, MA, USA) in buffer A (0.1% formic acid). Secondly, buffer B (84% acetonitrile and 0.1% Formic acid) was used to separate the peptides following a linear gradient, and the flow rate was 300 nl/min. The MS was performed in the positive ion mode in the study. To identify the most abundant precursor ions, MS analysis was dynamically carried out using the data-dependent top 10 method with a survey scan (300–1800 m/z) for higher-energy C-trap dissociation (HCD) fragmentation. The following parameters were applied to the entire MS detection method: maximum inject time: 10 ms; automatic gain control target: $3*10^6$; dynamic exclusion duration: 40 seconds; 70,000 mass resolution relative to m/z 200 and 17,500 resolution relative to m/z 200 for the HCD spectra; isolation window: 2 m/z; enzyme digestion mode: trypsin/p; variable modifications: oxidation (M); fixed modification: carbamidomethyl (C); and MS/MS tolerance: 20 ppm. The normalized collision energy (NCE) was 30 eV, and the underfill ratio, which was defined as the minimum percentage of the target value at the maximum fill time, was 0.1%. The peptide recognition mode was enabled. MaxQuant software (version: 1.5.3.17) was used for the identification and quantitation analysis of the raw MS data. For the identification and quantification of peptides and proteins, the UniProt human database (http://www.uniprot.org/), intensity Based Absolute Quantification and Label Free Quantitation algorithm were applied, and the false discovery rate were set to 1%. Proteins identified in more than 50% of the samples in each group were retained for further analysis. The raw data were not normalized in Label free quantitation. The DEPs in different samples was standardized by the Z-Score method when the cluster analysis was performed. The p values of the protein expressions between groups were calculated by the *t*-test. The proteins that presented a $|\log2(\text{fold change (FC)})| > 0.58$ and a p value < 0.05 were considered DEPs. The data sets in Tables 2 and 3 were arranged by the ratio of nAMD/control, PCV/control and PCV/nAMD.

Bioinformatics Analysis

The enriched pathways in the GO database and KEGG were used a bioinformatics analysis of the DEPs. The DEPs were arranged into the following GO categories: "CC", "BP" and "MF". PPIs play an important role in BP. Therefore, the IntAct molecular interaction database was applied to retrieve the PPI network information for the DEPs according to their gene symbols using STRING software (Version: 11.5). After downloading the results, the data of the PPI network were further analyzed and visualized using Cytoscape (Version: 3.9.1). All volcano plots in figures were created using R (version 3.4.1).

Table 2 Significantly Downregulated Proteins for Each Patient Group

Protein ID	Gene Name	Description	Peptides	FC	p-value
Control vs nAMD					
Q08188	TGM3	Protein-glutamine gamma-glutamyltransferase E	12	0.2	0.039
P15924	DSP	Desmoplakin	89	0.3	0.003
Q7Z7M0	MEGF8	Multiple epidermal growth factor-like domains protein 8	3	0.3	0.043
P31944	CASP14	Caspase-14	7	0.3	0.006
P04406	GAPDH	Glyceraldehyde-3-phosphate dehydrogenase	14	0.3	0.041
Q96PG2	MS4A10	Membrane-spanning 4-domains subfamily A member 10	2	0.3	0.033
P32119	PRDX2	Peroxiredoxin-2	9	0.4	0.019
P05089	ARG1	Arginase-1	5	0.4	0.039
Q02413	DSG1	Desmoglein-1	23	0.4	0.010
Q96P63	SERPINB12	Serpin B12	9	0.4	0.024
Control vs PCV					
Q96PG2	MS4A10	Membrane-spanning 4-domains subfamily A member 10	2	0.3	0.045
P61626	LYZ	Lysozyme C	8	0.4	0.045
P31944	CASP14	Caspase-14	7	0.4	0.029
Q13404	UBE2V1	Ubiquitin-conjugating enzyme E2 variant 1	2	0.5	0.011
O75223	GGCT	Gamma-glutamylcyclotransferase	4	0.5	0.002
Q08554	DSC1	Desmocollin-1	15	0.6	0.036
Q9NT99	LRRC4B	Leucine-rich repeat-containing protein 4B	3	0.6	0.020
Q8TF72	SHROOM3	Protein Shroom3	2	0.6	0.035
Q13410	BTN1A1	Butyrophilin subfamily 1 member A1	2	0.6	0.001
O95274	LYPD3	Ly6/PLAUR domain-containing protein 3	2	0.6	0.004
nAMD vs PCV					
A0M8Q6	IGLC7	Immunoglobulin lambda constant 7	4	0.4	0.001
Q6P387	C16orf46	Uncharacterized protein C16orf46	1	0.5	0.047
Q9NS15	LTBP3	Latent-transforming growth factor beta-binding protein 3	6	0.5	0.013
P81605	DCD	Dermcidin	3	0.6	0.044
Q9Y6R7	FCGBP	IgGFc-binding protein	52	0.6	0.019
Q5VU97	CACHD1	VWFA and cache domain-containing protein 1	4	0.6	0.026

ELISA Measurement

SAA4 (EH1155, FineTest, Wuhan, Hubei, China) was selected as the target protein, and the measured ELISA method was applied for the validation of SAA4 protein expression in the AH samples of individual patients, including 10 cataract patients, 10 treatment-naive nAMD patients and 10 treatment-naive PCV patients. The enrollment criteria and AH

Table 3 Summary of Human Aqueous Humor Samples

	LC-MS/MS Analysis				ELISA Validation			
Groups	**Control (n=10)**	**nAMD (n=10)**	**PCV (n=10)**	**p value**	**Control (n=10)**	**nAMD (n=10)**	**PCV (n=10)**	**p value**
Patient ID	C1-10	A1-10	P1-10		CV1-10	AV1-10	PV1-10	
Gender (M/F)	6/4	7/3	6/4	0.866	16/4	15/5	13/7	0.551
Age (ys)	71.00±8.68	68.80±10.55	68.20±9.86	0.796	71.50±9.40	73.20±9.44	71.05±10.59	0.767

collection method were consistent with those for the LC-MS/MS analysis mentioned above. In the SAA4 ELISA assay, we tested each sample in triplicate according to the SAA4 ELISA kit manufacturer's protocol (Figure 1).

Statistical Analysis

Statistical analyses were performed with the SPSS software (IBM SPSS Statistics 26, NY, USA). The chi-square test was used to compare the participants in terms of gender between the cataract, nAMD and PCV groups. Other clinical data were analyzed between groups using Student's test and one-way analysis of variance. For all analyses, $p < 0.05$ was considered statistically significant, and all p values were derived from 2-sided tests.

Results

Differentially Expressed Proteins (DEPs) Compared Between nAMD, PCV and Controls

The Liquid Chromatography with tandem mass spectrometry (LC-MS/MS) platform detected a total of 737 different proteins in the control, nAMD and PCV groups, of which 544 were quantifiable. There were 75 DEPs between the control and nAMD groups, including 19 downregulated proteins and 56 upregulated proteins. In total, 48 DEPs were found between the control and PCV groups, including 11 downregulated proteins and 37 upregulated proteins. Interestingly, in our analysis, we also identified seven DEPs (six downregulated proteins and one upregulated protein) in the PCV group that were significantly regulated relative to nAMD (Figure 2A and C–E). The DEP expression patterns were identified in a hierarchical cluster analysis between the different groups (Figure 3A, D and G). Proteomics analyses showed that a total of 631 proteins were present in all the groups (Figure 2B). To compare the proteins between different groups, we identified the DEPs which were unique to each group. Firstly, between the control and nAMD groups, the ten most upregulated proteins were P29401 (Transketolase), P01706 (Immunoglobulin lambda variable 2–11), P08571 (Monocyte differentiation antigen CD14), P07585 (Decorin), P01599 (Immunoglobulin kappa variable 1–17), P02675 (Fibrinogen beta chain), P02753 (Retinol-binding protein 4), P35542 (Serum amyloid A-4 protein), P07357 (Complement component C8 alpha chain) and P07360 (Complement component C8 gamma chain). Secondly, between the control and PCV groups, the ten most upregulated proteins were P01706 (Immunoglobulin lambda variable 2–11), P01861 (Immunoglobulin heavy constant gamma 4), A0A0B4J1V0 (Immunoglobulin heavy variable 3–15), P07360 (Complement component C8 gamma chain), P08571 (Monocyte differentiation antigen CD14), Q15223 (Nectin-1), P07357 (Complement component C8 alpha chain), P35542 (Serum amyloid A-4 protein), P00734 (Prothrombin) and P00748 (Coagulation factor XII) (Table 2). Additionally, the ten most downregulated DEPs between the different groups are shown in Table 3. Finally, since there were no previous comparative studies, we explored the DEPs between the nAMD and PCV groups. It is striking to note that only one upregulated DEP was observed in these two groups—Q06033 (Inter-alpha-trypsin inhibitor heavy chain H3) (Table 2). Although there were still several downregulated DEPs between the nAMD and PCV groups, including A0M8Q6 (Immunoglobulin lambda constant 7), Q6P387 (Uncharacterized protein C16orf46), Q9NS15 (Latent-transforming growth factor beta-binding protein 3), Q9Y6R7 (IgGFc-binding protein), P81605 (Dermcidin) and Q5VU97 (VWFA and cache-domain-containing protein 1), none of them were found to be statistically significant when compared with the controls (Tables 2 and 3).

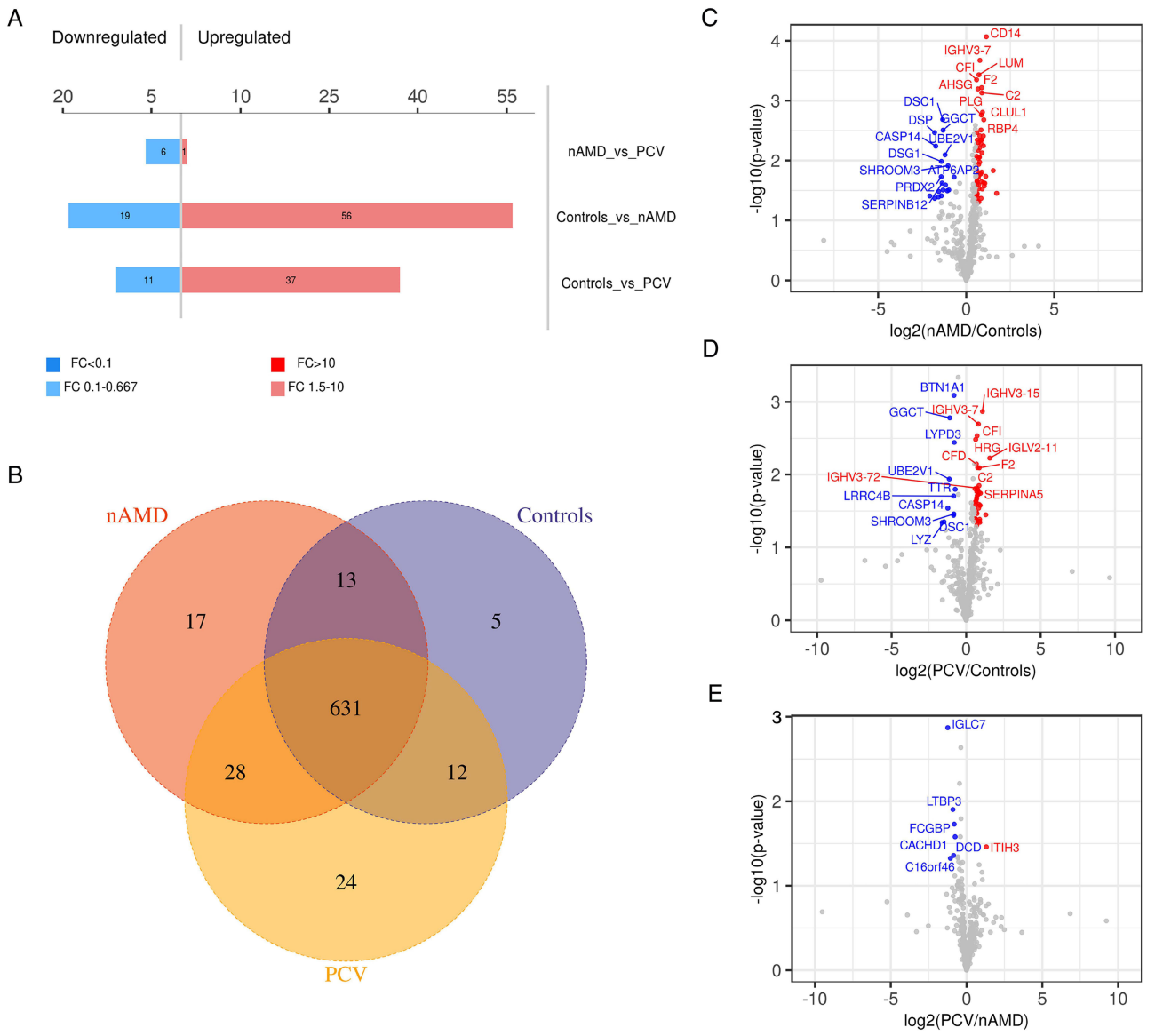

Figure 2 Venn diagram and Volcano plots of DEPs in different comparisons. (**A**) Up- and downregulated DEPs in different comparisons. (**B**) Venn diagram identifying 631 co-expressed DEPs among Control, nAMD and PCV, 5 unique DEPs in Control, 17 unique DEPs in nAMD and 24 unique DEPs in PCV. (**C**–**E**) Volcano plots showing the distribution of differentially expressed proteins in each comparison. The horizontal axis indicates the fold change (FC), the vertical axis indicates the p value. Red dots are upregulated DEPs, blue dots are downregulated DEPs, and gray dots are proteins without significant differential expression. (|log2(FC)| > 0.58; p value < 0.05).

Functional Analysis of the Identified nAMD- and PCV-Associated Proteins

Functional analysis of the significant DEPs in the AH samples was performed with the aim of revealing and visualizing a wide range of DEPs related to various biological pathways and processes. Cellular process, response to stimulus and biological regulation were the top three biological processes (BPs) in both the nAMD and PCV groups. The DEPs between nAMD and PCV were mostly involved in molecular function (MF) regulator, binding and catalytic activities. Furthermore, the extracellular region, cell part and cell were the highly enriched cellular components (CCs) in both groups. We further analyzed the DEPs between the control, nAMD and PCV groups, and the Gene ontology (GO) annotation results showed similar distributions (Figure 3B, C, E, F, H and I). The results of the Kyoto Encyclopedia of Genes and Genomes (KEGG) pathway annotation analysis between the groups are displayed in Figure 4A and B. Between the control and nAMD groups, there were 12 significant biological pathways. A total of 18 DEPs were enriched in the complement and coagulation cascades pathway (p=1.21E-09), 10 DEPs were related to the coronavirus disease COVID-19 (p=3.68E-05), and 6 DEPs were accumulated in the Staphylococcus aureus infection pathway (p=0.001).

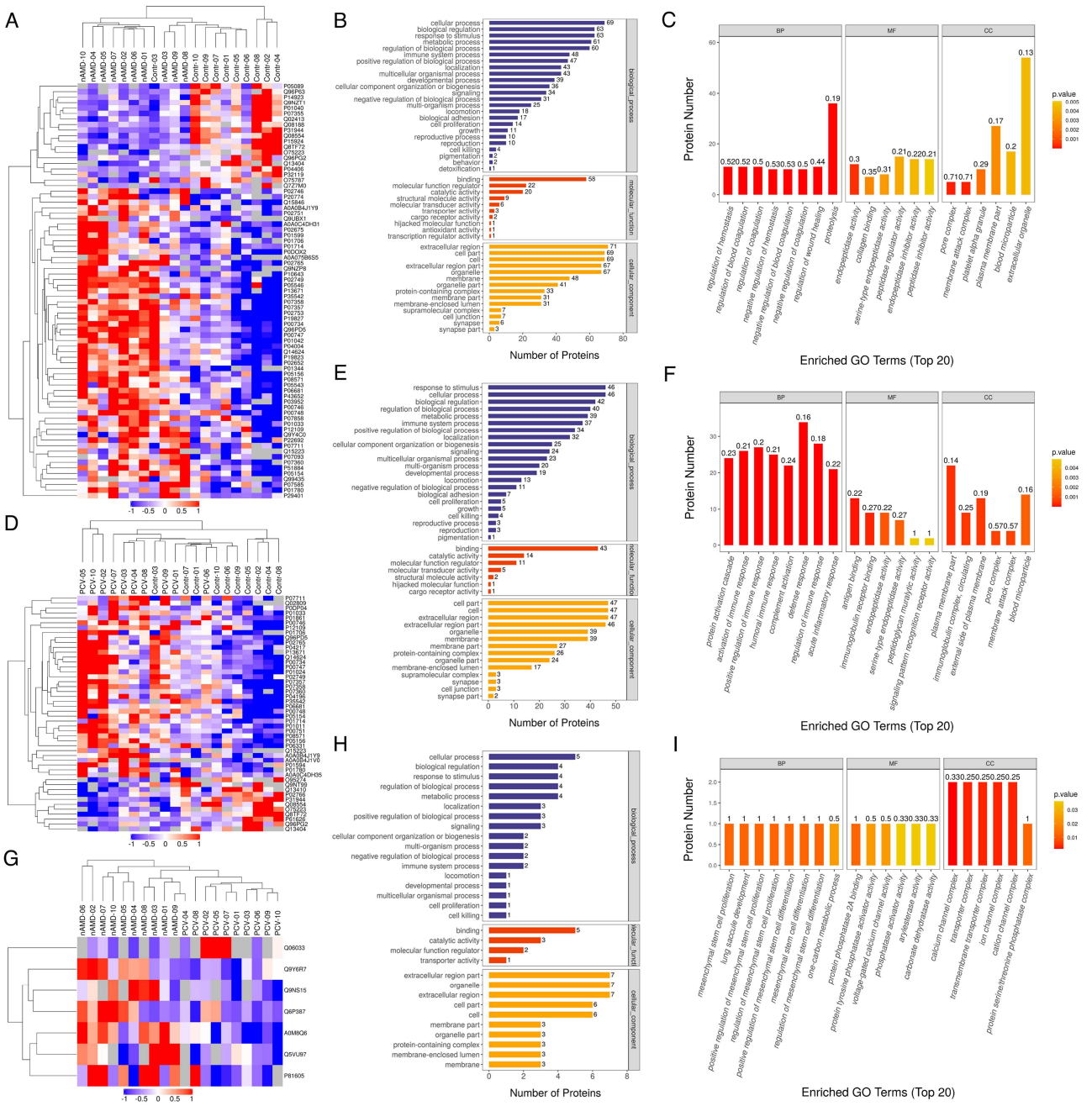

Figure 3 Heatmap and GO-term analysis of DEPs in different comparisons. Cluster analysis heatmap showing the DEPs in each comparison. Each column represents one biological replicate, each row represents a DEP. DEPs are presented in different colors in the heatmap after normalization. Red represents significantly upregulated proteins, blue represents significantly downregulated proteins, gray represents no quantitative information regarding the proteins. GO classification (Level 2) including BP, MF and CC, which differentiate in blue, red and Orange. The horizontal axis represents the number of DEPs in each functional classification. Top 20 enriched GO terms of significantly DEPs in each comparison are also shown. (**A**–**C**) Hierarchical cluster analysis and STRING GO-term enrichment of significantly DEPs between Control and nAMD groups. (**D**–**F**) Hierarchical cluster analysis and STRING GO-term enrichment of significantly DEPs between Control and PCV. (**G**–**I**) Hierarchical cluster analysis and STRING GO-term enrichment of significantly DEPs between nAMD and PCV. (|log2(FC)| > 0.58; P < 0.05).

Similarly, between the control and PCV group, the DEP-enriched pathways were the complement and coagulation cascades (p=2.41E-07), COVID-19 (p=1.01E-05) and Staphylococcus aureus infection pathways (p=9.38E-05) (Figure 4D and E). Moreover, between nAMD and PCV groups, there were DEPs enriched in some intriguing pathways, such as the nitrogen metabolism pathway (p=0.036), insulin resistance pathway (p=0.048) and diabetic cardiomyopathy pathway (p=0.116) (Figure 4G and H). The above mentioned pathways were mainly correlated with immunity- and

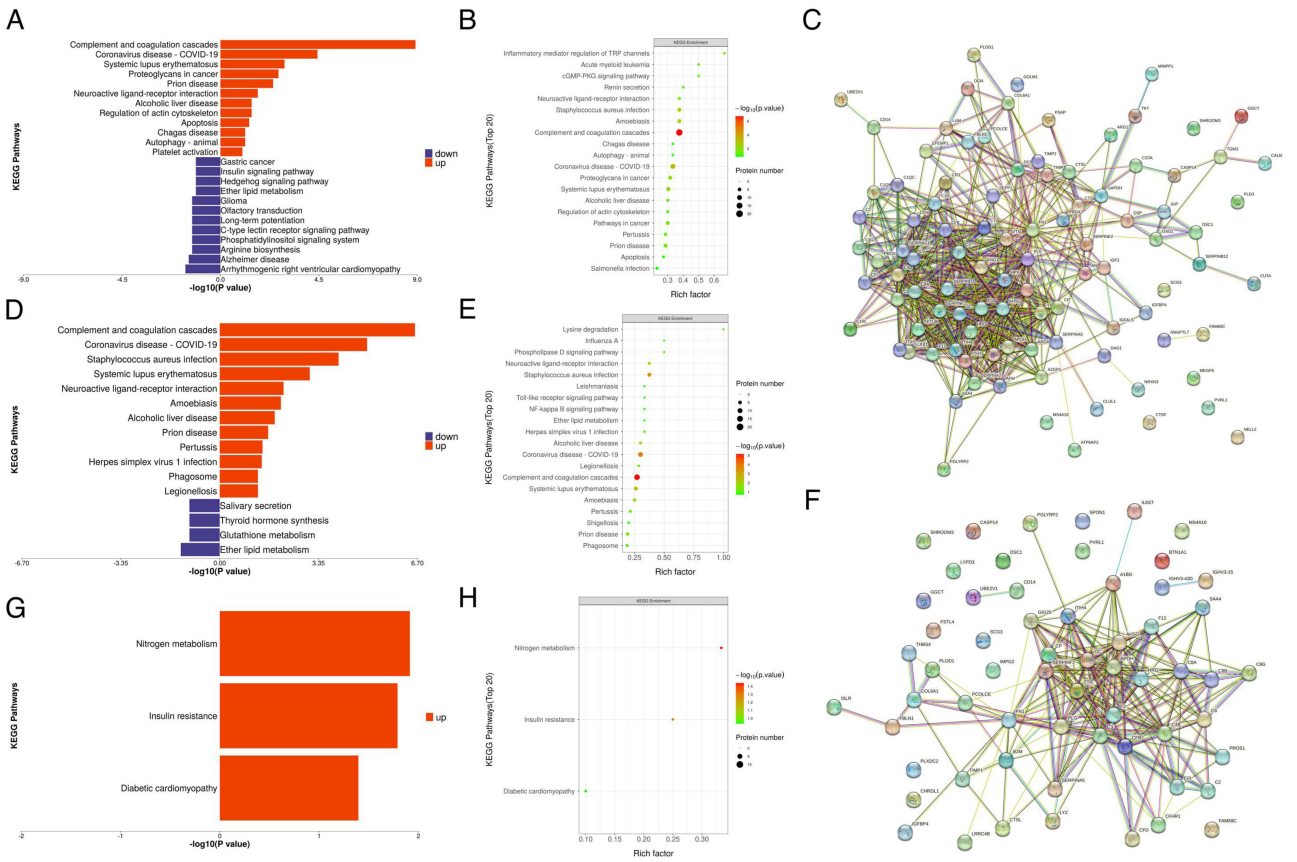

Figure 4 KEGG pathway enrichment and PPI network of DEPs in different comparisons. KEGG pathway enrichment analysis are represented with barplot and bubble plot, respectively. For upregulated DEGs, the top enriched pathways are represented in red. For downregulated DEGs, the top enriched pathways are represented in blue. In bubble plot, the horizontal axis is rich factor, the vertical axis is the name of the KEGG pathway. The bubble color scaled the enrichment score. Red represents more significant enrichment. The bubble size scaled the protein number. (**A**–**C**) KEGG pathway enrichment and PPI network displays in analysis of the up- and downregulated DEPs in Control vs nAMD group. (**D**–**F**) KEGG pathway enrichment and PPI network displays in analysis of the up- and downregulated DEPs in Control vs PCV group. (**G** and **H**) KEGG pathway enrichment finds in analysis of the up- and downregulated DEPs in nAMD vs PCV group.

inflammatory-related diseases.[26] To explore the interactions between DEPs from different groups, we further used the Search Tool for the Retrieval of Interacting Genes/Proteins (STRING) database and Cytoscape software to construct a Protein–protein interaction (PPI) network. As shown in Figure 4C and F, the proteins were closely connected with each other, and the central proteins in both nAMD and PCV were largely involved in immunity- and inflammatory-related diseases. The relationships between AH proteins and nAMD have been evaluated in recent studies.[27,28] Some of these proteins, such as P02765 (Alpha-2-HS-glycoprotein), were also detected in our study.[29] Furthermore, complement factors were the most common DEPs between the choroidal vasculopathies and controls (Tables 2 and 3). nAMD patients' vitreous fluid has been shown to contain higher levels of P00734 (prothrombin) compared with healthy controls, while P02749 (Beta-2-glycoprotein 1, APOH) is not expressed in neural retina and/or Retinal pigment epithelium (RPE)-choroid.[30,31] P35542 (Serum amyloid A-4 protein), a member of the SAA protein family, appears at the site of inflammation and is highly expressed in all inflammatory disorders. Thus far, there are no data on the association between SAA4 and nAMD or PCV in the literature. Therefore, further explorations are needed.

SAA4 as a Biomarker of nAMD and PCV

To verify the expression of SAA4 in the AH of the different groups, the proteomics results were validated using enzyme-linked immunosorbent assay (ELISA) with independent AH samples (10 in each group). There was no statistical significance with respect to differences in gender ($p = 0.551$) or age ($p = 0.767$) between these groups (Table 1). SAA4 expression in the nAMD (1.058±0.176 ng/mL) and PCV groups (1.174 ± 0.270 ng/mL) was significantly increased compared with that in the control

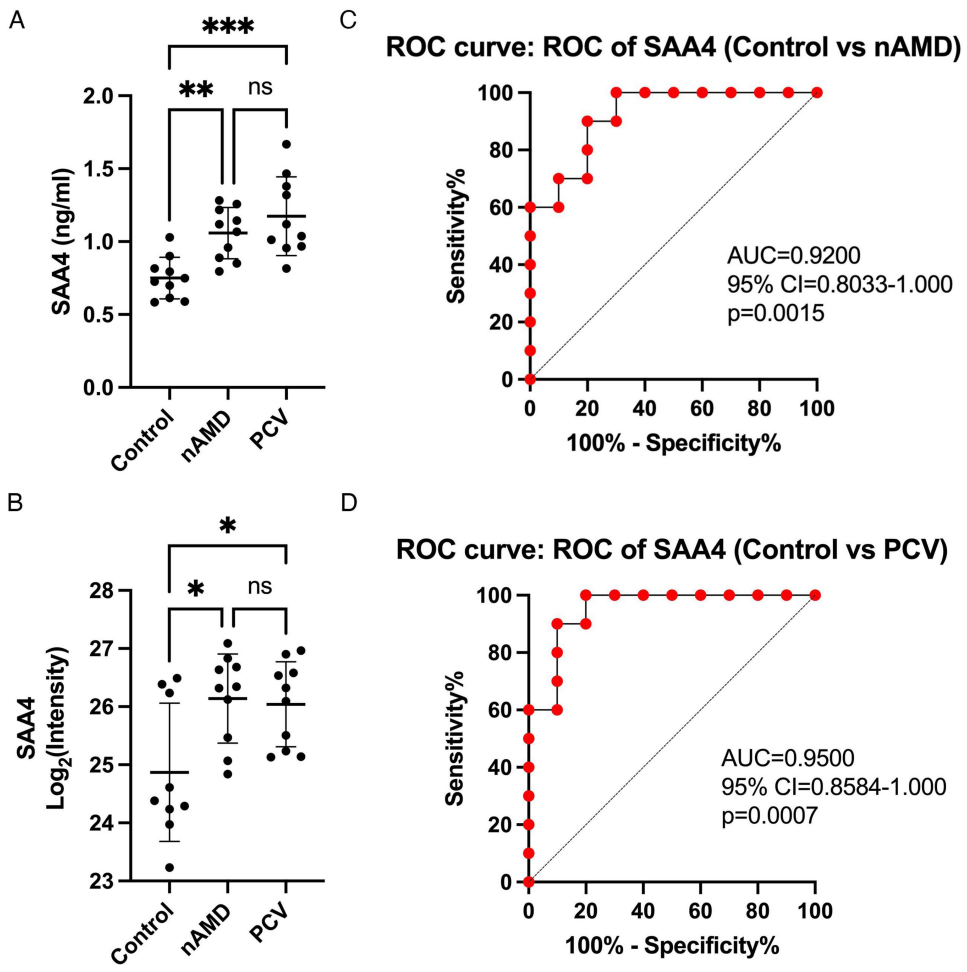

Figure 5 Validation of SAA4 and ROC analysis. (**A** and **B**) Comparison of SAA4 protein abundance measured by ELISA (**A**) with LC-MS/MS-based proteomics (**B**) measurements. (**C** and **D**) ROC curves depicting the classification power of SAA4. Data are presented as means ± SD; * indicates a p value < 0.05, **Indicates a p value < 0.01, ***Indicates a p value < 0.001, ns indicates not significant.

group (0.750±0.142 ng/mL) (p=0.006 and p=0.0002) (Figure 5A). Additionally, the ELISA data matched the proteomics-based expression pattern of SAA4 (p=0.014 and p=0.024) (Figure 5B). The receiver operating characteristic (ROC) curve demonstrated the strong discriminatory power of SAA4 (control vs nAMD, area under the curve (AUC) =0.9200; p=0.0015; 95% confidence interval (CI) = 0.8033 to 1.000) (control vs PCV, AUC =0.9500; p=0.0007; 95% CI = 0.8584 to 1.000) (Figure 5C and D).

Discussion

nAMD and PCV are common choroidal vasculopathies around the world. PCV is considered as a subtype of nAMD.[7] Patients with PCV may present with hemorrhage and/or exudation in the macular region, similar to those with nAMD. Typical nAMD can be managed using anti-VEGF drugs or in combination with photodynamic therapy that prevents CNV development, and this also applies to the current PCV treatment strategies. However, the effectiveness of these agents is not optimal, as approximately one-third of patients do not achieve the expected level of improvement in their best-corrected visual acuity, despite regular treatment.[11–13] Therefore, it is necessary to identify a novel common biomarker of these choroidal vasculopathies so as to facilitate the diagnosis of patients, clarify the pathogenesis, and guide potential treatment decisions. The AH might be an ideal tissue for the identification of biomarkers in clinics due to the ease of the material sampling process during intravitreal injection and cataract surgery.[32] Additionally, there is evidence to suggest that the proteome of AH is closely related to fundus diseases. Previous studies have examined alterations in the AH protein levels in diseases such as diabetic

retinopathy and pathologic myopia.[33,34] Furthermore, several MS-based proteomic studies on AMD, which used human AH, have already been conducted, though most of them have focused on nAMD.[27,28] A lack of comprehensive analysis means that it is difficult for researchers to further explore the common pathomechanisms of nAMD and PCV. Here, we independently compared the AH proteomes of nAMD, PCV and control patients.

In our study, a total of 737 proteins were identified, of which 544 were quantifiable. Through bioinformatics analysis, we found that the DEPs in nAMD and PCV, compared with the control group, were mainly concentrated in the extracellular region and involved in metabolic processes, stress and immune responses. Additionally, they had protein binding molecular functions. Similar numbers of proteins related to nAMD were found in another AH proteomics study, with the upregulated DEPs mainly involved in the complement activation pathway.[27] Complement system over-activation plays an important role in nAMD pathogenesis and development.[35] There were several specific proteins of interest in our study, such as C8A, C8G and CD14, which were distinctly upregulated in both the nAMD and PCV groups in comparison to the control group and were all immune proteins involved in complement activation and binding. In addition, the upregulation of immunoglobulin genes (IGLV2-11, IGKV1-17, IGHG4, IGHV3-15) in both the nAMD and PCV groups supports an adaptive, autoimmune response in AMD.[29] These findings are in line with previous reports of immune response activation in nAMD patients.[36,37] The complement and coagulation systems induce the proinflammatory and prothrombotic state involved in many diseases.[38,39] The upregulation of F2 and F12 in both the nAMD and PCV groups might provide us with good evidence to suggest that the complement and coagulation systems are critical.[40] In addition to the upregulated proteins overlapping both the nAMD and PCV groups, we also found some proteins that were elevated in the nAMD group alone. The plasma fibrinogen level, including Fibrinogen beta chain (FGB), was found to be significantly associated with late ARMD, which is consistent with The Blue Mountains Eye Study.[41] Decorin, a small leucine-rich proteoglycan, has been demonstrated to play a vital role in constituting the retinal microvasculature structure.[42] Retinol-binding protein 4 (RBP4) is an adipocyte-secreted protein and delivers vitamin A from the liver to RPE. A proteomics study conducted by Lim demonstrated that RBP4 could be used as a novel biomarker and therapeutic measure for nAMD.[43] Transketolase, the critical enzyme in the pentose phosphate pathway, was found to play a critical protective role on endoplasmic reticulum stress responses and cell survival in stressed human retina.[44] Although many studies have suggested that PCV is a special subtype of nAMD, there are still some differences in pathological mechanism between PCV and nAMD. In 2021, Van Dijk summarized three clinical subtypes of PCV: (1) PCV which is more closely related to nAMD; (2) PCV which is more closely related to BVN; and (3) PCV which is more closely related to polyp-like lesions. Type 1, associated with a normal to thin choroid, is more similar to typical nAMD, while types 2 and 3 may be correlated with a thick choroid (pachychoroid).[45] Subsequently, we further explored and compared the DEPs between the nAMD and PCV groups. Only one DEP was upregulated in PCV in comparison with nAMD. Inter-alpha-trypsin inhibitor heavy chain H3 (ITIH3) belongs to the group of inter-alpha trypsin inhibitors and plays a particularly important role in controlling immune responses, including inflammation.[46] Among the downregulated DEPs between nAMD and PCV, IGLC7, C16orf46 and FCGBP are related to immune and inflammatory responses.[47,48] Interestingly, the Dermcidin (DCD) and Latent-transforming growth factor beta-binding protein 3 (LTBP-3) expression levels were significantly decreased in the PCV group compared with the nAMD patients. DCD showed a close connectivity with the presence of peripapillary choroidal microvasculature dropout.[49] LTBP-3 controls the activation of TGF-beta by maintaining it. Osteosclerosis and osteoarthritis were observed in *Ltbp-3*$^{-/-}$ mice.[50] Based on the previous hypothesis regarding the differential pathological mechanisms of PCV and nAMD,[51,52] we selected DCD and LTBP-3 as novel DEPs in these two groups for further validation. Although these novel DEPs were identified in both nAMD and PCV, the downregulation of DCD and LTBP-3 was not reproduced using the ELISA assay (data not shown). Since immune dysregulation appeared to be an underlying alteration in nAMD and PCV in our data, we identified a new protein which show an increased expression of AH in both PCV and nAMD.

There are four SAA gene family members and two subgroups. The first subgroup, acute-phase SAA1 and SAA2, are related to high-density lipoprotein (HDL) and inflammation. SAA4 is the second subgroup. SAA3 expresses in mice but not in humans. The major source of SAA4 is the liver, where it has abundant expression, while some studies found that the abundant expression SAA4 can be specifically detected in tumorigenic tissues.[53,54] Not only inflammation but also atherosclerosis are considered as possible pathogenic mechanisms of PCV.[55] Notably, a recent study also indicated that

SAA4 expression is significantly increased in atherosclerosis, and it is a predictor and serologic biomarker of atheromatous lesions.[56] nAMD and RA are both degenerative conditions that share some pathomechanisms.[57] There is a positive correlation between SAA4 and rheumatoid factor, and SAA4 was identified as a novel RA diagnostic biomarker.[22] In addition to its involvement in inflammatory reactions, SAA4 also binds to HDL and very-low-density lipoprotein. When SAA accumulates in HDLs, it can impair the HDL anti-inflammatory capacity.[19] Therefore, the targeting of HDLs is considered as a potential therapeutic strategy for nAMD. However, there is no evidence to suggest that SAA4 has a potential effect on the pathogenesis of nAMD and PCV. In theory, the constitutive SAA4 level is not subject to remarkable alterations. Intriguingly, our results showed there was a significant increase in both the nAMD and PCV groups in comparison with the control. In this respect, SAA4 appears to be a good candidate for linking nAMD and PCV to inflammation and HDL. And SAA4 could be a biomarker of disease activity, the use of SAA4 during screening may improve prescreening diagnosis. PCV and nAMD can show clinical characteristics other than choroidal neovasculopathy, such as photoreceptor death and exudative subretinal/intraretinal fluid.[6] Moreover, the pathogenesis of CNV between nAMD and PCV is somewhat different. Drusen deposition and choroidal atrophy in the older population are characterized in nAMD, while pachychoroid, absence of drusen, and shallow irregular pigment epithelial detachment in the relatively younger population are characterized in PCV.[7] To date, many studies have demonstrated SAA proteins including SAA4 involved in cell death, angiogenesis, vascular remodeling, inflammation and lipid abnormalities, these pathological changes also involve and play an important role in pathogenesis of nAMD and PCV.[20,21,58–61] Although the role of SAA4, which was shown to be differentially expressed in our study, is not well understood in human disease, it worth further exploring. Due to limitations regarding the sample collection, especially the AH sample size for the PCV patients, our results need to be confirmed in future studies with larger sample sizes. Recently, Asia-Pacific Ocular Imaging Society PCV Workgroup recommended a set of practical diagnostic criteria for diagnosing PCV with high accuracy based on fundus and OCT results.[62] Mao explored the associations between AH concentrations of inflammatory cytokines and OCT findings.[63] Therefore, our next step should combine the obtained results with the clinical manifestations for further exploration.

In conclusion, this study indicated that the highly abundant DEPs found in AH proteins from common choroid neovasculopathy patients are mainly involved in immune-mediated responses. We not only confirmed the findings of previous studies but also suggested a specific proinflammatory proteomic profile for AH in both nAMD and PCV patients. SAA4 level alteration may serve as a common biomarker for nAMD and PCV. The comprehensive analysis of the AH proteome will provide insight into, and improve our understanding of, the pathological mechanisms of nAMD and PCV and aid in biomarker discovery for choroid neovasculopathies.

Data Sharing Statement

The data presented in this study are available on request from the corresponding author.

Institutional Review Board Statement

The study was conducted in accordance with the Declaration of Helsinki, and approved by the Ethics Committee of Tianjin Medical University Eye Hospital (No. 2021KY-12).

Informed Consent Statement

Informed consent was obtained from all subjects involved in the study.

Author Contributions

All authors made a significant contribution to the work reported, whether that is in the conception, study design, execution, acquisition of data, analysis and interpretation, or in all these areas; took part in drafting, revising or critically reviewing the article; gave final approval of the version to be published; have agreed on the journal to which the article has been submitted; and agree to be accountable for all aspects of the work.

Funding

The study was supported by National Natural Science Foundation of China (82171085); Key Project of Internet Cross-Border Integration Innovation and Technology of Tianjin (18ZXRHSY00210); Tianjin Key Medical Discipline (Specialty) Construction Project (TJYXZDXK-037A); Science and Technology Project of Tianjin Binhai New Area Health Commission (2022BWKQ011); the Natural Science Foundation of Tianjin City (22JCQNJC01220).

Disclosure

The authors declare no conflicts of interest in this work.

References

1. Mitchell P, Liew G, Gopinath B, Wong TY. Age-related macular degeneration. *Lancet*. 2018;392(10153):1147–1159. doi:10.1016/S0140-6736(18)31550-2
2. Wong WL, Su X, Li X, et al. Global prevalence of age-related macular degeneration and disease burden projection for 2020 and 2040: a systematic review and meta-analysis. *Lancet Global Health*. 2014;2(2):e106–e116. doi:10.1016/S2214-109X(13)70145-1
3. Chakravarthy U, Peto T. Current Perspective on Age-Related Macular Degeneration. *JAMA*. 2020;324(8):794–795. doi:10.1001/jama.2020.5576
4. Nashine S. Potential Therapeutic Candidates for Age-Related Macular Degeneration (AMD). *Cells*. 2021;10(9):2483. doi:10.3390/cells10092483
5. Mitchell SL, Ma C, Scott WK, et al. Plasma Metabolomics of Intermediate and Neovascular Age-Related Macular Degeneration Patients. *Cells*. 2021;10(11):3141. doi:10.3390/cells10113141
6. Teo K, Gillies M, Fraser-Bell S. The Use of Vascular Endothelial Growth Factor Inhibitors and Complementary Treatment Options in Polypoidal Choroidal Vasculopathy: a Subtype of Neovascular Age-Related Macular Degeneration. *Int J Mol Sci*. 2018;19(9):2611. doi:10.3390/ijms19092611
7. Cheung C, Lai T, Ruamviboonsuk P, et al. Polypoidal Choroidal Vasculopathy: definition. *Pathogenesis Diagnosis, Manage Ophthalmol*. 2018;125(5):708–724. doi:10.1016/j.ophtha.2017.11.019
8. Kikuchi M, Nakamura M, Ishikawa K, et al. Elevated C-reactive protein levels in patients with polypoidal choroidal vasculopathy and patients with neovascular age-related macular degeneration. *Ophthalmology*. 2007;114(9):1722–1727. doi:10.1016/j.ophtha.2006.12.021
9. Agrawal R, Balne PK, Wei X, et al. Cytokine Profiling in Patients With Exudative Age-Related Macular Degeneration and Polypoidal Choroidal Vasculopathy. *Invest Ophthalmol Vis Sci*. 2019;60(1):376–382. doi:10.1167/iovs.18-24387
10. Wu M, Xiong H, Xu Y, et al. Association between VEGF-A and VEGFR-2 polymorphisms and response to treatment of neovascular AMD with anti-VEGF agents: a meta-analysis. *Br J Ophthalmol*. 2017;101(7):976–984. doi:10.1136/bjophthalmol-2016-309418
11. Yerramothu P. New Therapies of Neovascular AMD-Beyond Anti-VEGFs. *Vision*. 2018;2(3):31. doi:10.3390/vision2030031
12. Gemenetzi M, Lotery AJ, Patel PJ. Risk of geographic atrophy in age-related macular degeneration patients treated with intravitreal anti-VEGF agents. *Eye*. 2017;31(1):1–9. doi:10.1038/eye.2016.208
13. Barış ME, Menteş J, Afrashi F, Nalçaçı S, Akkın C. Subgroups and Features of Poor Responders to Anti-Vascular Endothelial Growth Factor Treatment in Eyes with Neovascular Age-Related Macular Degeneration. *Turkish j Ophthalmol*. 2020;50(5):275–282. doi:10.4274/tjo.galenos.2020.38488
14. Yang S, Li T, Jia H. Targeting C3b/C4b and VEGF with a bispecific fusion protein optimized for neovascular age-related macular degeneration therapy. *Sci Transl Med*. 2022;14(647):eabj2177. doi:10.1126/scitranslmed.abj2177
15. Lavalette S, Raoul W, Houssier M, et al. Interleukin-1β inhibition prevents choroidal neovascularization and does not exacerbate photoreceptor degeneration. *Am J Pathol*. 2011;178(5):2416–2423. doi:10.1016/j.ajpath.2011.01.013
16. Izumi-Nagai K, Nagai N, Ozawa Y, et al. Interleukin-6 receptor-mediated activation of signal transducer and activator of transcription-3 (STAT3) promotes choroidal neovascularization. *Am J Pathol*. 2007;170(6):2149–2158. doi:10.2353/ajpath.2007.061018
17. Huang S, Mills L, Mian B, et al. Fully humanized neutralizing antibodies to interleukin-8 (ABX-IL8) inhibit angiogenesis, tumor growth, and metastasis of human melanoma. *Am J Pathol*. 2002;161(1):125–134. doi:10.1016/S0002-9440(10)64164-8
18. Sack GH. Serum Amyloid A (SAA) Proteins. *Subcell Biochem*. 2020;94:421–436. doi:10.1007/978-3-030-41769-7_17
19. Webb NR. High-Density Lipoproteins and Serum Amyloid A (SAA). *Curr Atheroscler Rep*. 2021;23(2):7. doi:10.1007/s11883-020-00901-4
20. Lv M, Xia YF, Li B, et al. Serum amyloid A stimulates vascular endothelial growth factor receptor 2 expression and angiogenesis. *J Physiol Biochem*. 2016;72(1):71–81. doi:10.1007/s13105-015-0462-4
21. De Buck M, Gouwy M, Wang JM, et al. The cytokine-serum amyloid A-chemokine network. *Cytokine Growth Factor Rev*. 2016;30:55–69. doi:10.1016/j.cytogfr.2015.12.010
22. Seok A, Lee HJ, Lee S, et al. Identification and Validation of SAA4 as a Rheumatoid Arthritis Prescreening Marker by Liquid Chromatography Tandem-mass Spectrometry. *Molecules*. 2017;22(5):805. doi:10.3390/molecules22050805
23. Sallustio F, Stasi A, Curci C. Renal progenitor cells revert LPS-induced endothelial-to-mesenchymal transition by secreting CXCL6, SAA4, and BPIFA2 antiseptic peptides. *FASEB J*. 2019;33(10):10753–10766. doi:10.1096/fj.201900351R
24. Shen C, Sun XG, Liu N, et al. Increased serum amyloid A and its association with autoantibodies, acute phase reactants and disease activity in patients with rheumatoid arthritis. *Mol Med Rep*. 2015;11(2):1528–1534. doi:10.3892/mmr.2014.2804
25. Mun S, Lee J, Park M, Shin J, Lim MK, Kang HG. Serum biomarker panel for the diagnosis of rheumatoid arthritis. *Arthritis Res Ther*. 2021;23(1):31. doi:10.1186/s13075-020-02405-7
26. Oikonomopoulou K, Ricklin D, Ward PA, Lambris JD. Interactions between coagulation and complement--their role in inflammation. *Semin Immunopathol*. 2012;34(1):151–165. doi:10.1007/s00281-011-0280-x
27. Rinsky B, Beykin G, Grunin M, et al. Analysis of the Aqueous Humor Proteome in Patients With Age-Related Macular Degeneration. *Invest Ophthalmol Vis Sci*. 2021;62(10):18. doi:10.1167/iovs.62.10.18
28. Kim TW, Kang JW, Ahn J, et al. Proteomic analysis of the aqueous humor in age-related macular degeneration (AMD) patients. *J Proteome Res*. 2012;11(8):4034–4043. doi:10.1021/pr300080s

29. Koss MJ, Hoffmann J, Nguyen N, et al. Proteomics of vitreous humor of patients with exudative age-related macular degeneration. *PLoS One*. 2014;9(5):e96895. doi:10.1371/journal.pone.0096895
30. Pool FM, Kiel C, Serrano L, Luthert PJ. Repository of proposed pathways and protein-protein interaction networks in age-related macular degeneration. *NPJ Aging Mechanisms Dis*. 2020;6:2. doi:10.1038/s41514-019-0039-5
31. Akter T, Annamalai B, Obert E, Simpson KN, Rohrer B. Dabigatran and Wet AMD, Results From Retinal Pigment Epithelial Cell Monolayers, the Mouse Model of Choroidal Neovascularization, and Patients From the Medicare Data Base. *Front Immunol*. 2022;13:896274. doi:10.3389/fimmu.2022.896274
32. López-Contreras AK, Martínez-Ruiz MG, Olvera-Montaño C, et al. Importance of the Use of Oxidative Stress Biomarkers and Inflammatory Profile in Aqueous and Vitreous Humor in Diabetic Retinopathy. *Antioxidants*. 2020;9(9):891. doi:10.3390/antiox9090891
33. Oruc Y, Celik F, Ozgur G, et al. Altered Blood And Aqueous Humor Levels Of Asprosin, 4-Hydroxynonenal, And 8-Hydroxy-Deoxyguanosine In Patients With Diabetes Mellitus And Cataract With And Without Diabetic Retinopathy. *Retina*. 2020;40(12):2410–2416. doi:10.1097/IAE.0000000000002776
34. Xue M, Ke Y, Ren X, et al. Proteomic analysis of aqueous humor in patients with pathologic myopia. *J Proteomics*. 2021;234:104088. doi:10.1016/j.jprot.2020.104088
35. Armento A, Schmidt TL, Sonntag I, et al. CFH Loss in Human RPE Cells Leads to Inflammation and Complement System Dysregulation via the NF-κB Pathway. *Int J Mol Sci*. 2021;22(16):8727. doi:10.3390/ijms22168727
36. Ebeling MC, Fisher CR, Kapphahn RJ, et al. Inflammasome Activation in Retinal Pigment Epithelium from Human Donors with Age-Related Macular Degeneration. *Cells*. 2022;11(13):2075. doi:10.3390/cells11132075
37. Park YG, Park YS, Kim IB. Complement System and Potential Therapeutics in Age-Related Macular Degeneration. *Int J Mol Sci*. 2021;22(13):6851. doi:10.3390/ijms22136851
38. de Bont CM, Boelens WC, Pruijn G. NETosis, complement, and coagulation: a triangular relationship. *Cell Mol Immunol*. 2019;16(1):19–27. doi:10.1038/s41423-018-0024-0
39. Afzali B, Noris M, Lambrecht BN, Kemper C. The state of complement in COVID-19. *Nat Rev Immunol*. 2022;22(2):77–84. doi:10.1038/s41577-021-00665-1
40. Göbel K, Eichler S, Wiendl H. The Coagulation Factors Fibrinogen, Thrombin, and Factor XII in Inflammatory Disorders-A Systematic Review. *Front Immunol*. 2018;9:1731. doi:10.3389/fimmu.2018.01731
41. Smith W, Mitchell P, Leeder SR, Wang JJ. Plasma fibrinogen levels, other cardiovascular risk factors, and age-related maculopathy: the Blue Mountains Eye Study. *Arch Ophthalmol*. 1998;116(5):583–587. doi:10.1001/archopht.116.5.583
42. Low S, Vaidya T, Gadde S, et al. Decorin Concentrations in Aqueous Humor of Patients with Diabetic Retinopathy. *Life*. 2021;11(12):1421. doi:10.3390/life11121421
43. Lim D, Lee H, Bokjun J. Increased level of retinol binding protein 4 in neovascular age-related macular degeneration. *Invest Ophthalmol Vis Sci*. 2015;56(7):5476.
44. Chen Y, Zhang T, Zeng S, et al. Transketolase in human Müller cells is critical to resist light stress through the pentose phosphate and NRF2 pathways. *Redox Biol*. 2022;54:102379. doi:10.1016/j.redox.2022.102379
45. van Dijk E, Mohabati D, Veselinovic S, Chung WH, Dijkman G, Boon C. The spectrum of polypoidal choroidal vasculopathy in Caucasians: clinical characteristics and proposal of a classification. Graefe's archive for clinical and experimental ophthalmology =. *Albrecht von Graefes Archiv fur klinische und experimentelle Ophthalmologie*. 2021;259(2):351–361. doi:10.1007/s00417-020-04844-z
46. Wickramasekara RN, Morrill S, Farhat Y, Smith SJ, Yilmazer-Hanke D. Glutathione and Inter-α-trypsin inhibitor heavy chain 3 (Itih3) mRNA levels in nicotine-treated Cd44 knockout mice. *Toxicology Reports*. 2018;5:759–764. doi:10.1016/j.toxrep.2018.06.010
47. Bracht T, Kleefisch D, Schork K, et al. Plasma Proteomics Enable Differentiation of Lung Adenocarcinoma from Chronic Obstructive Pulmonary Disease (COPD). *Int J Mol Sci*. 2022;23(19):11242. doi:10.3390/ijms231911242
48. Liu Q, Niu X, Li Y, et al. Role of the mucin-like glycoprotein FCGBP in mucosal immunity and cancer. *Front Immunol*. 2022;13:863317. doi:10.3389/fimmu.2022.863317
49. Lee SH, Jung JH, Park TK, et al. Proteome alterations in the aqueous humor reflect structural and functional phenotypes in patients with advanced normal-tension glaucoma. *Sci Rep*. 2022;12(1):1221. doi:10.1038/s41598-022-05273-0
50. Dabovic B, Chen Y, Colarossi C, Zambuto L, Obata H, Rifkin DB. Bone defects in latent TGF-beta binding protein (Ltbp)-3 null mice; a role for Ltbp in TGF-beta presentation. *J Endocrinol*. 2002;175(1):129–141. doi:10.1677/joe.0.1750129
51. Da M, Kumar M, Khetan V. Differential diagnosis between polypoidal choroidal vasculopathy (PCV) and Age-related macular degeneration (AMD) using Deep Neural Network. *Invest Ophthalmol Vis Sci*. 2020;61(7):2024.
52. Zhang X, Qiu B, Gong Z, Chen X, Wang Y, Nie Y. Differentially Regulated Apolipoproteins and Lipid Profiles as Novel Biomarkers for Polypoidal Choroidal Vasculopathy and Neovascular Age-Related Macular Degeneration. *Front Endocrinol (Lausanne)*. 2022;13:946327. doi:10.3389/fendo.2022.946327
53. Malle E, Sodin-Semrl S, Kovacevic A. Serum amyloid A: an acute-phase protein involved in tumour pathogenesis. Cellular and molecular life sciences. *CMLS*. 2009;66(1):9–26. doi:10.1007/s00018-008-8321-x
54. De Buck M, Gouwy M, Wang JM, et al. Structure and Expression of Different Serum Amyloid A (SAA) Variants and their Concentration-Dependent Functions During Host Insults. *Curr Med Chem*. 2016;23(17):1725–1755. doi:10.2174/0929867323666160418114600
55. Wong CW, Wong TY, Cheung CM. Polypoidal Choroidal Vasculopathy in Asians. *J Clin Med*. 2015;4(5):782–821. doi:10.3390/jcm4050782
56. Hrzenjak A, Artl A, Knipping G, Kostner G, Sattler W, Malle E. Silent mutations in secondary Shine-Dalgarno sequences in the cDNA of human serum amyloid A4 promotes expression of recombinant protein in Escherichia coli. *Protein Eng*. 2001;14(12):949–952. doi:10.1093/protein/14.12.949
57. Schnabolk G, Rohrer B, Simpson KN. Increased Nonexudative Age-Related Macular Degeneration Diagnosis Among Medicare Beneficiaries With Rheumatoid Arthritis. *Invest Ophthalmol Vis Sci*. 2019;60(10):3520–3526. doi:10.1167/iovs.18-26444
58. Siegmund SV, Schlosser M, Schildberg FA, et al. Serum Amyloid A Induces Inflammation, Proliferation and Cell Death in Activated Hepatic Stellate Cells. *PLoS One*. 2016;11(3):e0150893. doi:10.1371/journal.pone.0150893
59. de Beer MC, Yuan T, Kindy MS, Asztalos BF, Roheim PS, de Beer FC. Characterization of constitutive human serum amyloid A protein (SAA4) as an apolipoprotein. *J Lipid Res*. 1995;36(3):526–534. doi:10.1016/S0022-2275(20)39886-2

60. Thomas MJ, Sorci-Thomas MG. SAA: a link between cholesterol efflux capacity and inflammation? *J Lipid Res*. 2015;56(8):1383–1385. doi:10.1194/jlr.C061366
61. Fernández JA, Deguchi H, Elias DJ, Griffin JH. Serum amyloid A4 is a procoagulant apolipoprotein that it is elevated in venous thrombosis patients. *Res Pract Thromb Haemost*. 2019;4(2):217–223. doi:10.1002/rth2.12291
62. Cheung CMG, Lai TYY, Teo K, et al. Polypoidal Choroidal Vasculopathy: consensus Nomenclature and Non-Indocyanine Green Angiograph Diagnostic Criteria from the Asia-Pacific Ocular Imaging Society PCV Workgroup. *Ophthalmology*. 2021;128(3):443–452. doi:10.1016/j.ophtha.2020.08.006
63. Mao J, Chen N, Zhang S, et al. Association between inflammatory cytokines in the aqueous humor and hyperreflective foci on optical coherence tomography in patients with neovascular age-related macular degeneration and polypoidal choroidal vasculopathy. *Front Med*. 2022;9:973025. doi:10.3389/fmed.2022.973025